JPET MS # 93898

## Title Page

# Dominant role for calpain in thromboxane-induced neuromicrovascular endothelial cytotoxicity

Christiane Quiniou, Florian Sennlaub, Martin H. Beauchamp, Daniella Checchin, Isabelle Lahaie, Sonia Brault, Fernand Gobeil Jr., Mirna Sirinyan, Amna Kooli, Pierre Hardy, Alexey Pshezhetsky, Sylvain Chemtob

Centre de Recherche de l'Hôpital Ste-Justine, Departments of Pediatrics and Pharmacology, Université de Montréal (CQ, FS, MHB, DC, IL, SB, FGJr, MS, EK, PH, AP, SC); Department of Pharmacology and Therapeutics, McGill University, Montréal, Québec (DC, SB, MS, EK, SC); Department of Biochemistry, Université de Montréal, Québec (CQ); Department of Pharmacology , Université de Sherbrooke, Sherbrooke, Québec, Canada (FGJr).Institut National de la Santé et Recherche Médicale, Unite 598, Paris, France (FS)

JPET Fast Forward. Published on October 7, 2005 as DOI: 10.1124/jpet.105.093898
This article has not been copyedited and formatted. The final version may differ from this version.

JPET MS # 93898

Running title page

Running title: $TXA_2$-induced microvascular endothelial cell death

Correspondance author: Sylvain Chemtob, M.D., Ph.D., FRCPC; Department of Pediatrics, Ophthalmology and Pharmacology, Research Centre, Ste-Justine Hospital, 3175 Cote Ste-Catherine Montreal, Quebec H3T 1C5, Phone: 514-345-4931 #2978; Fax: 514-345-4801

Email:sylvain.chemtob@umontreal.ca

Abstract: 252 words

Introduction: 534 words

Discussion: 1103 words

Text pages: 34 pages

Tables: 0

Figures: 6

References: 53 references

Recommended section: Cellular and Molecular; Other: microvasculature, oxydative stress

The abbreviations used are: $TXA_2$, thromboxane $A_2$; TP, thromboxane receptor; DMEM, Dulbecco's modified Eagle's Medium; PBS, phosphate-buffered saline; Cyt C, cytochrome C; PVDF, polyvinylidene difluoride; MAPK, mitogen-activated protein kinase; erk, extracellular signal-regulated kinase; MEK, MAPK/erk kinase; LDH, Lactate dehydrogenase; MTT, 3-(4,5-dimethyl thiazol-2yl)-2,5-diphenyl tetrazolium bromide; $IP_3$, inositol triphosphate; U46619: 5-Heptenoic acid, 7-[6-(3-hydroxy-1-octenyl)-2-oxabicyclo[2.2.1]hept-5-yl]-[1R-[1α, 4α, 5β(Z), 6α, (1E,3S)]]-9,11-dedioxy-9α, 11 α,-methanolpoxy; CGS12970: 3-Methyl-2-(3-pyridyl)-1-indole-octonoic acid; L670596: ((-)6,8-difluoro-9-p-methylsulfonyl-benzyl-1,2,3,4-tetrahydrocarbazol-1-yl-acetic acid); U73122: 1-[6-((17β-3-Methoxyestro-1,3,5(10)-trien-17-yl)-amino)hexyl]-1H-pyrrole-2,5-dione; IBOP: [1S-[1 α, 2 α,(Z), 3β(1E,3S), 4 α,]]-7-[3-[3-hydroxy-4-(4-iodophenoxy)-1-butenyl]-7-oxabicyclo[2.2.1]hept-2-yl]-5-heptenoic acid

## ABSTRACT

$TXA_2$ is an important lipid mediator generated during oxidative stresses and implicated in ischemic neural injury. This autacoid was recently shown to partake in this process by directly inducing endothelial cytotoxicity. We explored the mechanisms for this $TXA_2$-evoked neural microvascular endothelial cell death. Stable $TXA_2$ mimetics U46619 (as well as I-BOP) induced a retinal microvascular degeneration in rat pups *in vivo,* on porcine retinal explants *ex vivo,* and death of porcine brain endothelial cells (in culture); $TXA_2$-dependence of these effects were corroborated by antagonism using the selective $TXA_2$ receptor blocker L670596. In all cases neurovascular endothelial cell death was prevented by pan-calpain and specific m-calpain inhibitors, but not by caspase 3 or pan-caspase inhibitors. Correspondingly, $TXA_2$ (mimetics) augmented generation of known active m-calpain (but not μ-calpain) form, and increased the activity of m-calpain (cleavage of fluorogenic substrate Suc-LLVY-AMC and of α-spectrin into specific fragments) but not of pan-caspase or specific caspase 3 (respectively, using SR-VAD-fmk and detecting its active 17 and 12 kDa fragments). Interestingly, these effects were PLC-dependent (associated with increase in $IP_3$ and inhibited by PLC blocker U73122) and required calcium but were not associated with increased intracellular calcium. U46619-induced calpain activation resulted in translocation of Bax to the mitochondria, loss of polarization of the latter (using potentiometric probe JC-1) and in turn release of cytochrome C into the cytosol and depletion of cellular ATP; these effects were all blocked by calpain inhibitors. Overall, this work identifies (specifically) m-calpain as a dominant protease in $TXA_2$–induced neurovascular endothelial cell death.

JPET Fast Forward. Published on October 7, 2005 as DOI: 10.1124/jpet.105.093898
This article has not been copyedited and formatted. The final version may differ from this version.



## INTRODUCTION

Increasing evidence points to neural microvascular endothelial dysfunction and cytotoxicity in ischemic brain injury (Lee and Lo, 2003); an analogous profile is well described in ischemic cardiopathies . This microangiopathy is a major feature of diabetic complications including retinopathy. Neurovascular endothelial cells seem particularly susceptible to the peroxidation involved in such types of injuries (Beauchamp et al., 2001; van Reyk et al., 2003). In the process of this oxidative stress cytosolic phospholipase $A_2$ is activated and ultimately leads to the predominant generation of thromboxane ($TXA_2$) over that of other eicosanoids (Ogletree, 1987; Chemtob et al., 1995); $TXA_2$ in turn exerts cellular effects by interacting with its receptor, named TP.

Cytotoxic effects of $TXA_2$ have largely been attributed to its hemodynamic actions elicited through vasoconstriction and platelet aggregation (FitzGerald et al., 1987). But more recently, direct toxicity in response to activation of the $TXA_2$ receptor has been uncovered in thymocytes (Ushikubi et al., 1993), throphoblasts (Yusuf et al., 2001), renal tubule epithelial cells (Jariyawat et al., 1997), ventricular myocytes (Shizukuda and Buttrick, 2002), as well as in (rat, porcine and human) neural microvascular endothelial cells (Lahaie et al., 1998; Beauchamp et al., 2001); in contrast, stimulation of receptors for related prostanoids $PGE_2$ and $PGF_{2\alpha}$ did not lead to toxicity. Of relevance, the major peroxidation products the isoprostanes exert neurovascular endothelial cytotoxicity via $TXA_2$/TP pathway (Beauchamp et al., 2001; Brault et al., 2003). Furthermore, an important role for $TXA_2$ has been demonstrated in retinal vasoobliteration associated with ischemic retinopathies prior to platelet aggregation (which itself generates $TXA_2$) (Beauchamp et al., 2002). This $TXA_2$/TP-induced neurovascular endothelial cell death is delayed by 12-18 h, albeit does not exhibit classical features of apoptosis such as

JPET Fast Forward. Published on October 7, 2005 as DOI: 10.1124/jpet.105.093898
This article has not been copyedited and formatted. The final version may differ from this version.



chromatin condensation, TUNEL positivity, and frequently observed caspase-dependence; accordingly, a role for other cysteine proteases may be inferred.

Caspases, calcium-dependent calpains, and cathepsins compose the three major groups of cysteine proteases. On the other hand, ubiquitous calpain isoforms Calp I (μ-calpain) and Calp II (m-calpain) are abundantly expressed in the central nervous system (Ray et al., 2003), and calpain activity is increased in the process of cell death applied to neurodegeneration and ischemic central nervous system events (Saito et al., 1993; Majno and Joris, 1995). Interestingly, calpain activity has mostly been associated with necrosis, while caspase activity is largely associated with classical apoptosis (Wang, 2000). However, whether calpains participate in $TXA_2$-induced endothelial cytotoxicity and the mechanisms involved in this process have yet to be described.

We therefore investigated the mechanisms of $TXA_2$-induced neurovascular endothelial cell death, with particular emphasis on the role of calpains; for this purpose established stable mimics of this prostanoid known to activate its TP receptor were used (U46619 and at times I-BOP). Our findings reveal that $TXA_2$ (mimics) elicited a neuroretinal microvascular degeneration *in vivo*, in tissue explants (*ex vivo*) and on primary neural endothelial cells (cultures) via a mechanism dependent upon calpain activity and was prevented specifically by m-calpain inhibitor, and mediated in turn by increased mitochondrial Bax/Bcl-2 ratio associated with loss of mitochondrial membrane polarity and consequent ATP depletion; in contrast, pan-caspase and more specifically caspase-3 activity and role were not involved. Thus, we hereby disclose an important mode of action of $TXA_2$ in eliciting neurovascular endothelial cytotoxicity.

**METHODS:**

JPET Fast Forward. Published on October 7, 2005 as DOI: 10.1124/jpet.105.093898
This article has not been copyedited and formatted. The final version may differ from this version.



*Chemicals and materials.* L670596 was a gift of Merck Frosst (Pointe-Claire, Quebec). The following materials were purchased: ceramide, DMSO, cycloheximide, staurosporine, Nonidet-P40 and MTT (Sigma Chemicals, St-Louis, MO); U46619 and I-BOP (Cayman Chemicals, Ann Arbor, MI); JC-1, valinomycin, Hoescht 33342 and prodpidium iodine from (Invitrogen, Burlington, ON); Calpain inhibitors IV and V, U73122 (Calbiochem, La Jolla, CA), and Z-DEVD-fmk caspase 3 inhibitor (R&D system, Minneapolis, MN). Other materials were purchased from Fisher Scientific (Montreal, Qc).

$TXA_2$-elicited effects were tested using stable analogs of the prostanoid, namely U46619 and I-BOP, both of which are known to stimulate specifically the TP receptor (Beauchamp et al., 2001); $TXA_2$-induced actions were further corroborated using the selective TP antagonist L670596 (Beauchamp et al., 2001).

*Animals.* Newborn Sprague-Dawley rats (Charles River, St-Constant, Québec, Canada) and 1 to 3 day old Yorkshire piglets (Fermes Ménard, L'Ange-Gardien, Québec, Canada) were used according to a protocol of the Hôpital Sainte-Justine Animal Care Committee and in accordance with regulations of the Canadian Council of Animal Care.

*Intravitreous injections.* Retinovascular degeneration was studied in rat pups as reported (Beauchamp et al., 2001). Rat pups (postnatal day 7) were injected intravitreously (1 µl [capillary injector]) with vehicle or U46619 in absence or presence of $TXA_2$ receptor blocker L670596 (estimated final concentration 1 µM [30 µl ocular volume] as described (Lahaie et al., 1998; Beauchamp et al., 2001)), pan-calpain inhibitor (Calp V, final concentration, 1 µM) or caspase 3 inhibitor Z-DEVD-fmk (final concentration, 50 µM); some preparations were treated with the pan-caspase inhibitor Z-VAD-fmk (50 µM). Rats were euthanized on postnatal day 10 and retinas isolated for endothelial cell staining with the TRITC-conjugated lectin griffonia

JPET Fast Forward. Published on October 7, 2005 as DOI: 10.1124/jpet.105.093898
This article has not been copyedited and formatted. The final version may differ from this version.



simplicifolia (Sigma-Aldrich, St Louis, MO). Retinas were visualized using a fluorescent Nikon Eclipse E800 microscope and photographed with a Nikon Digital Camera DMX1200. Vascular density was determined using a computer software (Image-Pro Plus 4.1; Media Cybernetics, Silver Spring, MD) as reported (Lahaie et al., 1998; Beauchamp et al., 2001).

*Retinal explants.* To ascertain that the vasculotoxic effects of $TXA_2$ are hemodynamic-independent and can be reproduced in different species, effects of the $TXA_2$ analog U46619 were tested on retinal explants of 1-3 day old pigs. Dissected retinas were cut into 5 $mm^2$ fragments, placed on a Whatman Track-Etch membrane and left to float on the surface of DMEM (2% FBS) culture medium at 37°C with 5 % $CO_2$ in 6 well plates (3 explants per membrane). Retinal explants were treated with vehicle or U46619 (1 μM) in the absence or presence of L670596 (1 μM), m-calpain inhibitor Calp IV (Angliker et al., 1992) ($k_2$ = 28,900 M-1s-1 (1 μM), pan-calpain inhibitor Calp V (Esser et al., 1994)(1 μM), or Z-DEVD-fmk (50 μM); some preparations were treated with the pan-caspase inhibitor Z-VAD-fmk (50 μM). μ-Calpain inhibitors are not yet available. After 3 days incubation the medium was removed and the explants were fixed at room temperature with formalin and permeabilized with ice cold 100% methanol. Tissues were washed thrice with 1% Triton X-100 in PBS and stained with 1:100 TRITC-lectin *grifonia simplicifolia* (in 1% Triton X) overnight. Explants were flat mounted and visualized with a fluorescent microscope and microvasculature quantified as described above for the intravitreal injection experiments.

*Cells.* Neural microvessels (≤25 μm) were isolated from piglet brains as previously detailed (Lahaie et al., 1998; Beauchamp et al., 2001; Beauchamp et al., 2002). Microvessels were suspended in selective endothelial growth media (Clonetics) and endothelial cells grown to confluence as reported (Lahaie et al., 1998; Beauchamp et al., 2001). Endothelial cells were

JPET Fast Forward. Published on October 7, 2005 as DOI: 10.1124/jpet.105.093898
This article has not been copyedited and formatted. The final version may differ from this version.



identified morphologically and by their positive reactivity to FVIII and negative reactivity to smooth muscle-specific actin and GFAP. Only low passage (<7) cell cultures were utilized.

*Cell viability assay*. Cells at approximately 80% confluence were reseeded in DMEM (without fetal bovine serum) for 18 to 24 h. Cells were incubated for up to 24-36 h with stable $TXA_2$ mimetics U46619 and at times with [1*S*-[1α,2α(*Z*),3β(1*E*,3*S**),4α]]-7-[3-[3-hydroxy-4-(4-iodophenoxy)-1-butenyl]-7-oxabicyclo[2.1.1]-hept-2-yl]-5-heptenoic acid (I-BOP) in the absence or presence of the selective $TXA_2$ receptor blocker L670596 (1 μM), Calp IV (1 μM), Calp V (1 μM), or caspase 3 inhibitor Z-DEVD-fmk (50 μM). Cell viability was determined by mitochondrial-dependent reduction of 3-(4,5-dimethyl thiazol-2yl)-2,5-diphenyl tetrazolium bromide (MTT) in wells containing approximately 60,000 cells as abundantly described (Lahaie et al., 1998; Beauchamp et al., 2001); reliability of assay was confirmed by cell counting. At the end of the experiment, MTT (0.5 mg/mL in PBS [pH 7.2]) was incubated with cells for 2 h at 37°C. The medium was then drained and the formazan product solubilized with acidified (40 mM HCl) isopropanol and optical density measured at 600 nm. Cell death was further established using membrane-impermeable DNA-binding dye, propidium iodide (PI) (McGahon et al., 1995) and released lactate dehydrogenase activity (LDH) (Lahaie et al., 1998; Beauchamp et al., 2001). LDH activity was measured spectrophotometrically at 340 nm as follows (Allain et al., 1973). Briefly, 800 μl of reaction medium (Tris-HCl 80 mM, NaCl 200 mM, NADH 0.2 mM) was added to 200 μl of the culture medium in a spectrophotometer cuvette. The reaction was started by adding 1.5 mM pyruvate (final). LDH content was calculated as (Δoptical density/Δtime [min]) x 9682 = units LDH/volume.

*Caspase and calpain activity*. Pan-caspase activity was determined using the fluorogenic substrate SR-VAD-fmk (BioMol) which fluoresces (red) upon binding to the active enzyme

JPET Fast Forward. Published on October 7, 2005 as DOI: 10.1124/jpet.105.093898
This article has not been copyedited and formatted. The final version may differ from this version.



(Grabarek et al., 2002). Essentially, microvascular endothelial cells were seeded on coverslips and treated as above; staurosporin (1 μM) was used as positive control activator of caspase. At the end of drug exposure period SR-VAD-fmk was added to the cell media for 1 h at 37°C. Cells were counterstained with Hoescht 33342. Cells were photographed under fluorescent microscopy and quantified with the Image Pro software described above. In addition, caspase 3 activity was determined by immunoreactivity of the 12 and 17 kDa caspase fragments; antibody to 12 and 17 kDa does not recognize full caspase 3 protein.

Calpain activity was measured using the fluorogenic synthetic substrate Suc-LLVY-AMC (Calpain activity kit, Calbiochem); hydrolysis of the substrate yields the fluorescent product AMC (Debiasi et al., 1999). In brief, microvascular cells (24 well plates) incubated for a given number of hours with U46619 were added with Suc-LLVY-AMC for 15 min at 37 °C, as described by the manufacturer. The formation of AMC was read with a fluorescence plate reader at the following wavelength settings, excitation 360-380 nm and emission 440-460 nm. Enzyme activity was measured as nmol of free AMC released/min/amount of total cell lysate protein. Calpain activity was also determined by specific cleavage of α-spectrin to yield a 145-150 immunoreactive fragment .

**Inositol phosphate measurements**.

Endothelial cells grown in 12 well plates were labelled with 1-2μCi/ml [$^{3}$H-myo inositol (17 Ci/mmol; Amersham Canada) overnight. The cells were preincubated in DMEM containing 10 mM LiCl with or without the phospholipase C (PLC) inhibitor U73122 (0.1 μM) or L670596 (1 μM) and treated with U46619 (0.1 μM) for 30 min at 37°C and the reaction was terminated by addition of 0.5 volume of NaOH (100 mM), followed by acidification with 2 mM formic acid.

JPET Fast Forward. Published on October 7, 2005 as DOI: 10.1124/jpet.105.093898
This article has not been copyedited and formatted. The final version may differ from this version.



Total inositol phosphates were separated by using Dowex AG1X8 (formate form) and 1.2 M ammonium formate in 0.1N formic acid as the eluant. Radioactivity of phosphoinositides was determined in liquid scintillation cocktail.

**Intracellular $Ca^{2+}$ measurements.**

Intracellular $Ca^{2+}$ concentration ($[Ca^{2+}]_i$ ) was measured using the fluorescent $Ca^{2+}$ indicator fura 2-AM as previously described. Cells were resuspended in HBSS with $Ca^{2+}$ (2,5 mM) and 1% fetal bovine serum and were then stimulated with U46619 (0.1 μM), EGTA (5 mM) or bradykinin (1 μM). $[Ca^{2+}]$i was determined in 2 ml of Fura 2-AM-loaded cell suspension and measured using a spectrofluorometer (model LS 50, Perkin-Elmer, Beaconsfield, UK); excitation wavelengths were 340 and 380 nm, and emission at 510 nm. Calibration of the fluorescent signal was determined on 2 ml of cell suspension by sequential addition of 0.2% Triton X-100 to obtain the maximal fluorescence ratio ($R_{max}$) and to 5 mM EGTA to obtain the minimal fluorescence ratio ($R_{min}$). Autofluorescence was determined by measuring fluorescence from non-loaded cells and subtracting it from the fluorescence produced by fura 2-loaded cells to calculate the fluorescence ratio R corresponding to the values produced at 340 and 380 nm. The $[Ca^{2+}]_i$ was calculated from the equation: $[Ca^{2+}]_i = K_d\,[(R - R_{min})/(R_{max} - R)](S_{f2}/S_{b2})$, where $K_d$ (224 nM) is the effective dissociation constant of the fura 2-$Ca^{2+}$ complex and $S_{f2}/S_{b2}$ is the ratio of fluorescence intensity at 380 nm wavelength in the presence of EGTA to that in the presence of Triton X-100 (Grynkiewicz et al., 1985).

**Western Blot**

JPET Fast Forward. Published on October 7, 2005 as DOI: 10.1124/jpet.105.093898
This article has not been copyedited and formatted. The final version may differ from this version.



Microvascular endothelial cells were treated with U46619 in absence or presence of inhibitors as described for cell viability assays. Twenty ug of protein from the lysate, mitochondrial or cytosol soluble fractions were loaded on SDS-Page 8 or 12 % and probed with Bax, $Bcl_2$, cytochrome C (Pharmingen), non-erythroid α-spectrin, active caspase-3 (Chemicon) latent and active m-calpain (Chemicon) and β-actin (Abcam).

**Mitochondrial and cytosol fraction isolation**

Cell fractionation was performed as described in detail (Gobeil et al., 2003). Stimulated cells were rinsed with PBS were concentrated by centrifugation (500 *g*). Cells were suspended in lysis buffer pH 7.4 (10 mM Tris-HCl, 10 mM NaCl, 3 $MgCl_2$, 30 mM sucrose) and homogenized with a glass homogenizer (300 strokes); lysate was centrifuged at 700 *g* for 10 min at 4ºC to remove nuclei and debris, and the supernatant re-centrifuged at 10,000 *g* for 15 min. The mitochondrial-containing pellet was resuspended in phosphate buffer and utilized for corresponding experiments (see below), while the supernatant was centrifuged again at 120,000 *g* 1 h to obtain the S100 cytosolic fraction.

**Mitochondrial membrane potential**

Mitochondrial membrane depolarization was determined using the potentiometric probe JC-1 (Smiley et al., 1991). JC-1 selectively enters the polarized mitochondrias and is driven by the mitochondrial membrane electrochemical gradient; in polarized membrane it forms red fluorescent aggregates and when depolarized JC-1 stays dispersed as a monomer and fluoresces in green. Microvascular endothelial cells were split in 6 well plates and treated as described above for viability assays. Following the 24 h incubation period, cells were trypsinized,

JPET Fast Forward. Published on October 7, 2005 as DOI: 10.1124/jpet.105.093898
This article has not been copyedited and formatted. The final version may differ from this version.



centrifuged and resuspended in 500 µl PBS. JC-1 (1 µM) was added for 15 min at 37ºC; valinomycin (100 nM) was used as a positive control of mitochondrial depolarization. Monomers and aggregates of JC-1 were detected in the FL1 and FL2 channels respectively with a FACSCalibur (Becton Dickinson; San José; CA). For microscopic visualization, cells were photographed as described above.

**ATP assay**

ATP content was determined using a commercial kit (Calbiochem). Microvascular endothelial cells were splitted in 12-wells plates starved and treated. Cells were suspended in boiling 100 mM Tris-HCl pH 7.75, 4 mM EDTA buffer, for 10 min to inactivate released ATPases. Suspension was centrifuged and cooled. Fifty µl of cell suspension was mixed with 50 µl Hepes buffer and 25 µl luciferin-luciferase solution. ATP was determined by measuring the light generated, using the following formula described in the manufacturer's manual: D-luciferin + ATP-$Mg^{2+}$ + $O_2$ luciferase $\rightarrow$ Oxyluciferin + AMP + $CO_2$ + Ppi-$Mg^{2+}$ + light.

**Statistical analysis**

Data were analyzed by one- or two-way ANOVA factoring for treatment and/or time or concentration; comparison among means was analyzed by Tukey-Kramer method. Statistical significance was set at $P < 0.05$. Values are presented as mean ± SEM.

**RESULTS**:

**$TXA_2$-induced neural microvascular degeneration: role of calpain**

JPET Fast Forward. Published on October 7, 2005 as DOI: 10.1124/jpet.105.093898
This article has not been copyedited and formatted. The final version may differ from this version.



U46619 injected intravitreally to rat pups induced a significant decrease in retinal vessel density (Fig. 1). These effects were prevented by the selective $TXA_2$ receptor blocker L670596 and by the pan-calpain inhibitor (Calp V), but not by the caspase 3 inhibitor Z-DEVD-fmk; the pan-caspase inhibitor Z-VAD-fmk was also inefficient. To ascertain that the observed effects of $TXA_2$ were not simply due hemodynamic changes ($TXA_2$-induced vasoconstriction and ensued ischemia) and to show that they can be reproduced in higher species, experiments were conducted on porcine retinal explants. U46619 caused a marked loss (degeneration) of microvasculature (compared to vehicle-treated controls) (Fig. 2) equivalent to that detected *in vivo* (Fig. 1); I-BOP induced similar effects (not shown). Retinal microvascular density was relatively preserved by co-treatment with L670596, pan-calpain inhibitor Calp V, and m-calpain inhibitor Calp IV (Fig. 2); (μ-calpain inhibitors are not yet available).

**Cytotoxic effects of $TXA_2$ and role of calpain specifically apply to the neural microvascular endothelium**

To ascertain that the cytotoxic effects of $TXA_2$ and thus far presumed (pharmacological) role of calpain specifically apply to the neural microvascular endothelium, the latter was studied on primary neurovascular endothelial cell cultures. $TXA_2$ analogs, U46619 as well as I-BOP, induced a concentration- and time-dependent decrease in cell viability, determined by MTT assay and LDH release (Fig. 3A,B) (and confirmed by direct cell counting); accordingly, cellular PI incorporation was increased by U46619 (Fig. 3D). This U46619-triggered cytotoxicity was largely prevented by the selective $TXA_2$ receptor blocker L670596, Calp IV and CalpV, as well as by the PLC and PKC inhibitors, respectively U73122 and calphostin-C (Fig. 3B,C,D);

JPET Fast Forward. Published on October 7, 2005 as DOI: 10.1124/jpet.105.093898
This article has not been copyedited and formatted. The final version may differ from this version.



whereas Z-DEVD-fmk (or Z-VAD-fmk [not shown]) was ineffective, consistent with *in vivo* and *ex vivo* observations (Figs. 1 and 2).

**$TXA_2$-mediated changes in caspase and calpain activities**

Effects of $TXA_2$ (mimetic) on caspase and calpain activities were specifically studied. U46619 (at 6 h and 24 h) failed to activate caspase 3 in contrast to staurosporin as determined by increased immunoreactivity of the 17 and 12 kDa fragments (Fig. 4C). In addition, pan-caspase activity determined using the enzyme-binding fluorescent substrate SR-VAD-fmk did not reveal any activity upon treatment (24 h, as well as 12 h [not shown]) with U46619 (Fig. 4A,B); (the positive control) staurosporin (Gao et al., 2000) readily evoked caspase activation which was inhibited by Z-DEVD-fmk.

In contrast, U46619 evoked a significant increase in the formation of the 58 kDa m-calpain active fragment within 8 h (Fig. 5A) (Weber et al., 2004; Park and Ferreira, 2005); whereas μ-calpain was unaltered. Generation of m-calpain active fragment was inhibited by treatment with PKC and PLC inhibitors respectively calphostin-C and U73122; correspondingly, U46619 evoked an increase in inositol phosphate generation which was blocked by U73122 (Fig. 5B). Calpain activity (at 6 h) was also found to increase dose-dependently in response to U46619 as shown using the fluorogenic synthetic substrate Suc-LLVY-AMC (Fig. 5C,D); this effect was again blocked by U73122 and calphostin-C, and as expected by L670596 and Calp IV. This increase in calpain activity was further confirmed by induced hydrolysis of cytoskeletal α-spectrin which generates a Calp IV-sensitive 145-150 kDa specific fragment of spectrin detectable by Western blot (Fig. 5E).

JPET Fast Forward. Published on October 7, 2005 as DOI: 10.1124/jpet.105.093898
This article has not been copyedited and formatted. The final version may differ from this version.



Calpain activity is calcium-dependent (Sato and Kawashima, 2001). Interestingly however, U46619 does not elicit net calcium transients in neurovascular endothelial cells (Lahaie et al., 1998) as presently corroborated (Fig. 5F). On the other hand calpain activation can be PKC-dependent (Fig. 5A,D) as long as cellular calcium is maintained. Indeed depletion of calcium stores with thapsigargin and concurrent extracellular calcium chelation (with EGTA) precluded U46619-induced calpain activation (Fig. 5D).

**$TXA_2$-induced mitochondrial dysfunction**

Cytotoxicity secondary to calpain activation is reported to occur in a number of instances via sequential activation of Bax leading to mitochondrial dysfunction (Chen et al., 2002; Liu et al., 2004). We therefore determined the immunoreactivity of the pro-cell death protein Bax relative to that of the anti-cell death protein Bcl-2 in cytosol and mitochondria of endothelial cells treated with the $TXA_2$ mimetic U46619. Bax expression in mitochondria increased while that in cytosol decreased over time after stimulation with U46619 consistent with a translocation of Bax to the mitochondria (Fig. 6A). This led to a corresponding rise in Bax/Bcl-2 ratio in the mitochondria, which was virtually abrogated by L670596, Calp IV and Calp V (Fig. 6A). Accordingly, U46619 caused (at 18 and 24 h) mitochondrial membrane depolarization (appearance of green and loss of red fluorescence [colors are superimposed in Fig. 6B]), associated with release of cytochrome C in the cytosol (Fig. 6C) and ATP depletion (Fig. 6D). U46619-induced changes in mitochondrial function were markedly attenuated by the mitochondrial permeability transition pore blocker bongkrekic acid (Halestrap and Brennerb, 2003), as well as by L670596, Calp IV and Calp V (Fig. 6B); valinomycin served as a positive control.

JPET Fast Forward. Published on October 7, 2005 as DOI: 10.1124/jpet.105.093898
This article has not been copyedited and formatted. The final version may differ from this version.



## DISCUSSION

$TXA_2$ is an important lipid autacoid which participates in oxidative stress-induced neuroretinal injury (Lahaie et al., 1998; Beauchamp et al., 2001; Brault et al., 2003). This property of $TXA_2$ has recently been emphasized in relation to ischemic complications associated with cyclooxygenase-2 inhibitors . In addition to well-known hemodynamic impairment induced by $TXA_2$ (FitzGerald et al., 1987), direct cytotoxic effects upon activation of its receptor have now been described, and these appear to contribute to neurovascular degeneration (Beauchamp et al., 2001; Brault et al., 2003). However the mechanisms for $TXA_2$-induced neurovascular endothelial cytotoxicity is not known. We therefore conducted the present study to explore such mechanisms. Our findings reveal that $TXA_2$ (mimetics and activators of the TP receptor) elicits a neurovascular endothial injury *in vivo*, *ex vivo* and directly on primary (cultured) cells via a mechanism dependent upon calpain, but not caspase activity, prevented by selective TP blocker and specifically by m-calpain inhibitor, and mediated in turn by an apparent translocation of Bax to the mitochondria associated with loss of mitochondrial membrane polarity and consequent cellular ATP depletion. These observations disclose a previously undescribed mechanism in neurovascular endothelial cytotoxicity elicited by the major autacoid $TXA_2$ and mediated mostly by m-calpain.

A dominant feature in this study is the role of calpain without that of caspase in $TXA_2$-induced neurovascular endothelial cell death. The $TXA_2$ mimetic U46619 elicited early m-calpain activation (within 6 h) detected by distinct techniques (Fig. 5A,C-E), whereas pan-caspase and caspase 3 activation were not detected at early and later times (6 and 24 h) (Fig. 4A-C). More importantly, calpain and more specifically m-calpain inhibitors but not caspase 3 or

pan-caspase inhibitors (Beauchamp et al., 2001), prevented (to a similar extent) microvascular degeneration *in vivo* and *ex vivo*, as well as endothelial cell death *in vitro* (Figs. 1-3). Findings point to a major role for m-calpain in $TXA_2$-evoked neural microvascular endothelial cell death. Cell death often but not exclusively involves an interaction between calpains and caspases (Neumar et al., 2003; Rami, 2003). For instance the degradation of the endogenous calpain inhibitor calpastatin by caspase could potentiate the combined cytotoxic effects of calpains and caspases (Wang et al., 1998); but this explanation is unlikely since calpastatin immunoreactivity was unaltered in the first 24 h response to U46619 (data not shown). Another potential mechanism of interaction between these protease systems could be through the release of cytochrome C in the cytosol following calpain-induced disruption of mitochondrial integrity, which in turn would predictably sequentially activate caspases 9 and 3 (Vindis et al., 2004). However, neither activation nor a role for caspases in U46619-induced neurovascular endothelial cell death could be detected (Figs. 1,2,3C,4). Perhaps the explanation may lie in the inactivation of caspases 9 and 3 by calpains despite the release of cytochrome C, as reported for certain types of cell death (Chua et al., 2000) consistent with present observations (Fig. 6C).

Cell death induced by calpains is for the most part believed to occur by causing mitochondrial dysfunction and ensued ATP depletion (Liu et al., 2004) by modifying the expression of pro- and anti-cytotoxic small proteins such as Bax and Bcl-2 (Gao et al., 2000) on mitochondrial membrane (Cory et al., 2003) following kinase activation (Tsuruta et al., 2004),(Nomura et al., 2003) or proteolysis (Chen et al., 2001); calpain-dependent cell death can also take place through the direct presence of calpain (-like) activity at the mitochondria which impairs the permeability transition pore function (Gores et al., 1998). Although we cannot rule out the latter, our findings support a $TXA_2$-induced increase in Bax/Bcl-2 ratio at the

mitochondria and associated loss of mitochondrial membrane polarity and cellular ATP depletion, which are prevented by calpain inhibitors (Fig. 5A,B,D).

Mechanisms for $TXA_2$-induced activation of calpain appear complex and somewhat unexpected. Other than in humans, in other species $TXA_2$ acts on a single receptor homologous to the human TPα receptor (Kinsella, 2001). TPα can couple to Gs, $G_{q/11}$ or $G_{12/13}$ (Walsh et al., 2000), but apparently not to $G_i$; correspondingly, pertussis toxin did not effect calpain activation. Stimulation of Gs would lead to an increase in cAMP, but the latter is primarily involved in cell survival including of the central nervous system (Cui and So, 2004)), and thus exerts effects opposite to those we observed (Figs. 1-3). $G_{12/13}$ effects are mostly mediated by Rho GTPases (Kurose, 2003), which are however downstream of calpains (Sato and Kawashima, 2001). On the other hand our findings support coupling of TP to $G_{q/11}$, which leads to activation of phospholipase C to generate $IP_3$ (Fig. 5B). But surprisingly, although calpains are well known to be activated by a rise in intracellular $Ca^{++}$ (Sato and Kawashima, 2001), U46619 (and I-BOP) do not elicit $Ca^{++}$ transients in neurovascular endothelial cells ((Lahaie et al., 1998) and Fig. 5F). However as long as intracellular $Ca^{++}$ concentrations are not depleted other mechanisms partake in calpain activation (Fig. 5A,C,D-F) such as phosphorylation (Sato and Kawashima, 2001). Of relevance, diacylglycerol generated concurrently with $IP_3$ during phospholipase C catalysis activates protein kinase C (Exton, 1993), which in turn can phosphorylate and activate calpain . Indeed, both the inhibitors of phospholipase C and PKC respectively U73122 and calphostin-C, prevented U46619-induced activation of m-calpain (active fragment and activity) (Fig. 5A,D) and ensuing endothelial cell death (Fig. 3C).

Endothelial cytotoxicity and ensued impaired angiogenesis in response to $TXA_2$ has been reported in a number of studies (Beauchamp et al., 2001; Ashton et al., 2003; Brault et al., 2003;

Ashton and Ware, 2004). However, endothelial cells of various origins respond differently; for example, dermal and aortic endothelial cells are not susceptible to $TXA_2$ (Beauchamp et al., 2001; Beauchamp et al., 2002; Brault et al., 2003), whereas on cornea U46619 induces angiogenesis in the presence (but not in the absence) of fibroblast growth factor (Daniel et al., 1999). Dissimilar actions of $TXA_2$ on different endothelial cells likely reflect the heterogeneity of endothelium as the same receptor couples to different signalling partners in different cells (Gudermann et al., 1996); notably for instance, one would expect distinct phenotypes and corresponding functions in glomerular and brain endothelium.

In summary we have identified a major mechanism in neurovascular endothelial cell death in response to $TXA_2$, specifically (and principally) m-calpain. In this process we have also uncovered a previously unreported role for calpain in endothelial cell death secondary to this important mediator of oxidant stress, namely $TXA_2$ (Beauchamp et al., 2001; Beauchamp et al., 2002; Brault et al., 2003). Because preservation of microvasculature especially in the salvageable ischemic penumbra is important, our findings provide an additional explanation for the efficacy of calpain inhibitors in ischemic encephalopathies and retinopathies (Tamada et al., 2002; Rami, 2003).

**ACKNOWLEDGMENTS :**

*We are thankful to Mrs. H. Fernandez for her technical assistance.

**REFERENCES**:

Allain CC, Henson CP, Nadel MK and Knoblesdorff AJ (1973) Rapid single-step kinetic colorimetric assay for lactate dehydrogenase in serum. *Clin Chem* **19**:223-227.

Angliker H, Anagli J and Shaw E (1992) Inactivation of calpain by peptidyl fluoromethyl ketones. *J Med Chem* **35**:216-220.

Ashton AW, Ware GM, Kaul DK and Ware JA (2003) Inhibition of tumor necrosis factor alpha-mediated NFkappaB activation and leukocyte adhesion, with enhanced endothelial apoptosis, by G protein-linked receptor (TP) ligands. *J Biol Chem* **278**:11858-11866.

Ashton AW and Ware JA (2004) Thromboxane A2 receptor signaling inhibits vascular endothelial growth factor-induced endothelial cell differentiation and migration. *Circ Res* **95**:372-379.

Beauchamp MH, Marrache AM, Hou X, Gobeil F, Jr., Bernier SG, Lachapelle P, Abran D, Quiniou C, Brault S, Peri KG, Roberts J, 2nd, Almazan G, Varma DR and Chemtob S (2002) Platelet-activating factor in vasoobliteration of oxygen-induced retinopathy. *Invest Ophthalmol Vis Sci* **43**:3327-3337.

Beauchamp MH, Martinez-Bermudez AK, Gobeil F, Jr., Marrache AM, Hou X, Speranza G, Abran D, Quiniou C, Lachapelle P, Roberts J, 2nd, Almazan G, Varma DR and Chemtob

S (2001) Role of thromboxane in retinal microvascular degeneration in oxygen-induced retinopathy. *J Appl Physiol* **90**:2279-2288.

Brault S, Martinez-Bermudez AK, Marrache AM, Gobeil F, Jr., Hou X, Beauchamp M, Quiniou C, Almazan G, Lachance C, Roberts J, 2nd, Varma DR and Chemtob S (2003) Selective neuromicrovascular endothelial cell death by 8-Iso-prostaglandin F2alpha: possible role in ischemic brain injury. *Stroke* **34**:776-782.

Chemtob S, Hardy P, Abran D, Li DY, Peri K, Cuzzani O and Varma DR (1995) Peroxide-cyclooxygenase interactions in postasphyxial changes in retinal and choroidal hemodynamics. *J Appl Physiol* **78**:2039-2046.

Chen M, He H, Zhan S, Krajewski S, Reed JC and Gottlieb RA (2001) Bid is cleaved by calpain to an active fragment in vitro and during myocardial ischemia/reperfusion. *J Biol Chem* **276**:30724-30728.

Chen M, Won DJ, Krajewski S and Gottlieb RA (2002) Calpain and mitochondria in ischemia/reperfusion injury. *J Biol Chem* **277**:29181-29186.

Chua BT, Guo K and Li P (2000) Direct cleavage by the calcium-activated protease calpain can lead to inactivation of caspases. *J Biol Chem* **275**:5131-5135

.

Cory S, Huang DC and Adams JM (2003) The Bcl-2 family: roles in cell survival and oncogenesis. *Oncogene* **22**:8590-8607.

Cui Q and So KF (2004) Involvement of cAMP in neuronal survival and axonal regeneration. *Anat Sci Int* **79**:209-212.

Daniel TO, Liu H, Morrow JD, Crews BC and Marnett LJ (1999) Thromboxane A2 is a mediator of cyclooxygenase-2-dependent endothelial migration and angiogenesis. *Cancer Res* **59**:4574-4577.

Debiasi RL, Squier MK, Pike B, Wynes M, Dermody TS, Cohen JJ and Tyler KL (1999) Reovirus-induced apoptosis is preceded by increased cellular calpain activity and is blocked by calpain inhibitors. *J Virol* **73**:695-701.

Esser RE, Angelo RA, Murphey MD, Watts LM, Thornburg LP, Palmer JT, Talhouk JW and Smith RE (1994) Cysteine proteinase inhibitors decrease articular cartilage and bone destruction in chronic inflammatory arthritis. *Arthritis Rheum* **37**:236-247.

Exton JH (1993) Role of G proteins in activation of phosphoinositide phospholipase C. *Adv Second Messenger Phosphoprotein Res* **28**:65-72.

FitzGerald GA, Healy C and Daugherty J (1987) Thromboxane A2 biosynthesis in human disease. *Fed Proc* **46**:154-158.

Gao Y, Yokota R, Tang S, Ashton AW and Ware JA (2000) Reversal of angiogenesis in vitro, induction of apoptosis, and inhibition of AKT phosphorylation in endothelial cells by thromboxane A(2). *Circ Res* **87**:739-745.

Gobeil F, Jr., Bernier SG, Vazquez-Tello A, Brault S, Beauchamp MH, Quiniou C, Marrache AM, Checchin D, Sennlaub F, Hou X, Nader M, Bkaily G, Ribeiro-da-Silva A, Goetzl EJ and Chemtob S (2003) Modulation of pro-inflammatory gene expression by nuclear lysophosphatidic acid receptor type-1. *J Biol Chem* **278**:38875-38883.

Gores GJ, Miyoshi H, Botla R, Aguilar HI and Bronk SF (1998) Induction of the mitochondrial permeability transition as a mechanism of liver injury during cholestasis: a potential role for mitochondrial proteases. *Biochim Biophys Acta* **1366**:167-175.

Grabarek J, Ardelt B, Du L and Darzynkiewicz Z (2002) Activation of caspases and serine proteases during apoptosis induced by onconase (Ranpirnase). *Exp Cell Res* **278**:61-71.

Grynkiewicz G, Poenie M and Tsien RY (1985) A new generation of Ca2+ indicators with greatly improved fluorescence properties. *J Biol Chem* **260**:3440-3450.

Gudermann T, Kalkbrenner F and Schultz G (1996) Diversity and selectivity of receptor-G protein interaction. *Annu Rev Pharmacol Toxicol* **36**:429-459.

Halestrap AP and Brennerb C (2003) The adenine nucleotide translocase: a central component of the mitochondrial permeability transition pore and key player in cell death. *Curr Med Chem* **10**:1507-1525.

Jariyawat S, Takeda M, Kobayashi M and Endou H (1997) Thromboxane A2 mediates cisplatin-induced apoptosis of renal tubule cells. *Biochem Mol Biol Int* **42**:113-121.

Kinsella BT (2001) Thromboxane A2 signalling in humans: a 'Tail' of two receptors. *Biochem Soc Trans* **29**:641-654.

Kurose H (2003) Galpha12 and Galpha13 as key regulatory mediator in signal transduction. *Life Sci* **74**:155-161.

Lahaie I, Hardy P, Hou X, Hassessian H, Asselin P, Lachapelle P, Almazan G, Varma DR, Morrow JD, Roberts LJ, 2nd and Chemtob S (1998) A novel mechanism for vasoconstrictor action of 8-isoprostaglandin F2 alpha on retinal vessels. *Am J Physiol* **274**:R1406-1416.

Lee SR and Lo EH (2003) Interactions between p38 mitogen-activated protein kinase and caspase-3 in cerebral endothelial cell death after hypoxia-reoxygenation. *Stroke* **34**:2704-2709.

Liu X, Van Vleet T and Schnellmann RG (2004) The role of calpain in oncotic cell death. *Annu Rev Pharmacol Toxicol* **44**:349-370.

Majno G and Joris I (1995) Apoptosis, oncosis, and necrosis. An overview of cell death. *Am J Pathol* **146**:3-15.

McGahon AJ, Martin SJ, Bissonnette RP, Mahboubi A, Shi Y, Mogil RJ, Nishioka WK and Green DR (1995) The end of the (cell) line: methods for the study of apoptosis in vitro. *Methods Cell Biol* **46**:153-185.

Neumar RW, Xu YA, Gada H, Guttmann RP and Siman R (2003) Cross-talk between calpain and caspase proteolytic systems during neuronal apoptosis. *J Biol Chem* **278**:14162-14167.

Nomura M, Shimizu S, Sugiyama T, Narita M, Ito T, Matsuda H and Tsujimoto Y (2003) 14-3-3 Interacts directly with and negatively regulates pro-apoptotic Bax. *J Biol Chem* **278**:2058-2065.

Ogletree ML (1987) Overview of physiological and pathophysiological effects of thromboxane A2. *Fed Proc* **46**:133-138.

Park SY and Ferreira A (2005) The generation of a 17 kDa neurotoxic fragment: an alternative mechanism by which tau mediates beta-amyloid-induced neurodegeneration. *J Neurosci* **25**:5365-5375.

Rami A (2003) Ischemic neuronal death in the rat hippocampus: the calpain-calpastatin-caspase hypothesis. *Neurobiol Dis* **13**:75-88.

Ray SK, Matzelle DD, Sribnick EA, Guyton MK, Wingrave JM and Banik NL (2003) Calpain inhibitor prevented apoptosis and maintained transcription of proteolipid protein and myelin basic protein genes in rat spinal cord injury. *J Chem Neuroanat* **26**:119-124.

Saito K, Elce JS, Hamos JE and Nixon RA (1993) Widespread activation of calcium-activated neutral proteinase (calpain) in the brain in Alzheimer disease: a potential molecular basis for neuronal degeneration. *Proc Natl Acad Sci U S A* **90**:2628-2632.

Sato K and Kawashima S (2001) Calpain function in the modulation of signal transduction molecules. *Biol Chem* **382**:743-751.

Shizukuda Y and Buttrick PM (2002) Protein kinase C-zeta modulates thromboxane A(2)-mediated apoptosis in adult ventricular myocytes via Akt. *Am J Physiol Heart Circ Physiol* **282**:H320-327.

Smiley ST, Reers M, Mottola-Hartshorn C, Lin M, Chen A, Smith TW, Steele GD, Jr. and Chen LB (1991) Intracellular heterogeneity in mitochondrial membrane potentials revealed by a J-aggregate-forming lipophilic cation JC-1. *Proc Natl Acad Sci U S A* **88**:3671-3675.

Tamada Y, Fukiage C, Daibo S, Yoshida Y, Azuma M and Shearer TR (2002) Involvement of calpain in hypoxia-induced damage in rat retina in vitro. *Comp Biochem Physiol B Biochem Mol Biol* **131**:221-225.

Tsuruta F, Sunayama J, Mori Y, Hattori S, Shimizu S, Tsujimoto Y, Yoshioka K, Masuyama N and Gotoh Y (2004) JNK promotes Bax translocation to mitochondria through phosphorylation of 14-3-3 proteins. *Embo J* **23**:1889-1899.

Ushikubi F, Aiba Y, Nakamura K, Namba T, Hirata M, Mazda O, Katsura Y and Narumiya S (1993) Thromboxane A2 receptor is highly expressed in mouse immature thymocytes and mediates DNA fragmentation and apoptosis. *J Exp Med* **178**:1825-1830.

van Reyk DM, Gillies MC and Davies MJ (2003) The retina: oxidative stress and diabetes. *Redox Rep* **8**:187-192.

Vindis C, Teli T, Cerretti DP, Turner CE and Huynh-Do U (2004) EphB1-mediated cell migration requires the phosphorylation of paxillin at Tyr-31/Tyr-118. *J Biol Chem* **279**:27965-27970.

Walsh M, Foley JF and Kinsella BT (2000) Investigation of the role of the carboxyl-terminal tails of the alpha and beta isoforms of the human thromboxane A(2) receptor (TP) in mediating receptor:effector coupling. *Biochim Biophys Acta* **1496**:164-182.

Wang KK (2000) Calpain and caspase: can you tell the difference?, by kevin K.W. WangVol. 23, pp. 20-26. *Trends Neurosci* **23**:59.

Wang KK, Posmantur R, Nadimpalli R, Nath R, Mohan P, Nixon RA, Talanian RV, Keegan M, Herzog L and Allen H (1998) Caspase-mediated fragmentation of calpain inhibitor protein calpastatin during apoptosis. *Arch Biochem Biophys* **356**:187-196.

Weber H, Jonas L, Huhns S and Schuff-Werner P (2004) Dysregulation of the calpain-calpastatin system plays a role in the development of cerulein-induced acute pancreatitis in the rat. *Am J Physiol Gastrointest Liver Physiol* **286**:G932-941.

Yusuf K, Smith SD, Levy R, Schaiff WT, Wyatt SM, Sadovsky Y and Nelson DM (2001) Thromboxane A(2) limits differentiation and enhances apoptosis of cultured human trophoblasts. *Pediatr Res* **50**:203-209.

**FOOTNOTES:**

C Quiniou is a recipient of a schorlarship from the Heart and Stroke Foundation of Canada. F. Gobeil is a recipient of a Junior 1 scholarship from the FRSQ and a researcher of the Canada Foundation for Innovation. S. Chemtob is a Canada Research Chair recipient. This study was supported in parts by grants from the Canadian Institute of Health Research, the Heart and Stroke Foundation of Québec, and the March of Dimes.

Figure legends

Fig. 1. $TXA_2$-mediated retinal microvascular vasoobliteration. Rat pups on postnatal day 7 were injected intravitreously (1 μl) with vehicle or U46619 in absence or presence of $TXA_2$ receptor antagonist L670596 (estimated final concentration 1 μM [30 μl ocular volume] as described (Lahaie et al., 1998; Beauchamp et al., 2001; Beauchamp et al., 2002)), pan-calpain inhibitor (Calp V, final concentration, 1 μM) or Z-DEVD-fmk caspase 3 inhibitor (final concentration, 50 μM). Retinas were removed on postnatal day 10 and endothelium stained with TRITC-conjugated lectin *griffonia simplicifolia* to determine vessel density. A) Representative retinal flat mounts depicting vascular network. Note decreased vessel density after U46619, which is noticeably prevented by L670596 and Calp V. B) Compiled vessel density of retinas treated as described above. Values are mean ± SEM of 3-4 experiments. * $P < 0.05$ compared to all other values without asterisks.

Fig. 2. Microvascular degeneration induced on retinal explants by U46619. Porcine retinas were incubated for 3 days with vehicle or U46619 (0.1 μM) without or with L670596 (1 μM), Calp V (1 μM), Calp IV (1 μM) or Z-DEVD-fmk (50 μM) as described in Methods. Vascular network was revealed with TRITC-conjugated lectin *griffonia simplicifolia.* A) Representative flat mounts of incubated retinas treated with different compounds. Note marked decrease in vessel density induced by U46619 alone. B) Histographic representation of compiled vessel density data of tissues treated as described above. Values are mean ± SEM of 3-4 experiments. * $P < 0.05$ compared to all other values without asterisks.

JPET Fast Forward. Published on October 7, 2005 as DOI: 10.1124/jpet.105.093898
This article has not been copyedited and formatted. The final version may differ from this version.



**Fig. 3.** A) Time and concentration dependence of effects of $TXA_2$ analogs U46619 and I-BOP on porcine neurovascular endothelial cell viability determined by MTT assay (see Methods). B) LDH activity in endothelial cell media at given times following treatment with U46619 (0.1 μM) with or without L670596 (1 μM). C) Cell viability determined by MTT assay after 24 h treatment with vehicle or U46619 (0.1 μM) with or without (1 μM) L670596, Calp IV, Calp V, calphostin-C, U73122 or Z-DEVD-fmk (50 μM). D) Propidium iodide (PI, red) incorporation after 24 h treatment of cells with indicated treatments at concentrations described in (C). Cells were counterstained with Hoescht 33342 (blue); inhibitors alone did not affect PI incorporation. Representative photomicrographs are shown on the left, and quantification in histogram format is presented on the right. Values are mean ± SEM of 3-6 experiments. * $P < 0.05$ compared to other values without asterisks.

**Fig. 4.** Caspase activity in porcine neurovascular endothelial cells treated with U46619. A) Representative micrographs of pan-caspase activity determined using the fluorogenic substrate SR-VAD-fmk; cells were counterstained with Hoescht 33342. Cells were treated with U46619 (0.1 μM) for 12 h (not shown) or 24 h, or with staurosporin (1 μM) for 1 h without or with caspase 3 inhibitor Z-DEVD-fmk (50 μM). Green fluorescence was not detected after treatment with U46619 but was with staurosporin (positive control), which was prevented by Z-DEVD-fmk. B) Histographic representation of pan-caspase activity determined using SR-VAD-fmk. Values are mean ± SEM of 3 experiments. * $P < 0.01$ compared to other values without asterisks. C) Activated caspase 3 fragments determined by Western blot (representative of 3 experiments). U46619 (0.1 μM) did not increase immunoreactivity to the caspase 3 fragments; the positive

JPET Fast Forward. Published on October 7, 2005 as DOI: 10.1124/jpet.105.093898
This article has not been copyedited and formatted. The final version may differ from this version.



control staurosporin (1 μM; 1 h) induced an increase in caspase 3 fragment immunoreactivity. Values are mean ± SEM of 3 experiments. * $P < 0.05$ compared to other values without asterisks.

**Fig 5.** Calpain activation and activity. A) Calpain activation detected by Western Blot of 58 kDa fragment resulting from the U46619 (0.1 μM)-induced hydrolysis of the 80 kDa latent m-calpain at 8 h in the absence or presence of the PKC inhibitor calphostin (1 μM), PLC inhibitor U73122 (1 μM) and the $TXA_2$ receptor antagonist L670596 (1 μM). Representative blots are found on left, while compiled data is presented in histogram format on the right. B) Inositol phosphate generation in response to U46619 (0.1 μM) in the absence or presence of L670596 (1 uM) or U73122 (1 μM). C) Calpain activity, determined using the fluorogenic substrate Suc-LLVY-AMC (see Methods) in response to U46619 (at 6 h). D) Calpain activity measured as in (B) in the absence or presence of calphostin-C (1 μM), U73122 (1 μM), L670596 (1 μM) or Calp IV (1 μM). E) Representative (of 3 experiments) calpain activity detected by Western blot of a 145-150 kDa specific fragment of α-spectrin resulting from hydrolysis; 250 kDa band represents the full α-spectrin. β-actin was used as loading control. Endothelial cells were treated for 6 or 18 h with U46619 (1 μM) without or with Calp IV (1 μM). U46619 induced a robust increase in immunoreactivity of the 145-150 kDa fragment of α-spectrin. F) Net peak calcium transients in neurovascular endothelial cells in response to (1 μM) U46619 and bradykinin with or without EGTA (1 mM). One notes absent response to U46619. Values are mean ± SEM of 3-4 experiments. * $P < 0.05$ compared to other values without asterisks.

**Fig. 6.** $TXA_2$-mediated mitochondrial dysfunction of porcine neurovascular endothelial cells. A)

U46619 (0.1 μM)-induced translocation of Bax to the mitochondria. Drug concentrations were as described in Fig. 3. Values are mean ± SEM of 3-4 experiments. B) Mitochondrial depolarization evoked by U46619 (0.1 μM) in presence or absence of L670596 (1 μM), Calp V (1 μM), or the adenine nucleotide translocator of the mitochondrial permeability transition pore bongkrekic acid (50 μM); mitochondrial membrane depolarization was determined using the potentiometric probe JC-1 (see Methods). Some preparations were treated with valinomycin (100 nM) a known inducer of mitochondrial depolarization. Photomicrographs are merged images (orange-yellow) of polarized (red) and depolarized (green) mitochondrias. Representative micrographs are shown on the left, and compiled data in histogram format presented on the right; inhibitors alone did not affect mitochondrial depolarization. Values are mean ± SEM of 3 experiments. * $P < 0.05$ compared to other values without asterisks. C) Effects of U46619 (0.1 μM) on cytochrome C (Cyt C) release in the cytosol. The 15 kDa cytochrome C was detected in the cytosol by immunoblotting (representative of 3 experiments); β-actin (lower band) was used as control. Cells were treated as indicated; concentration of inhibitors is presented in (B). Note increase in cytosolic cytochrome C upon treatment with U46619 alone and prevented by inhibitors. D) ATP cell content as a function of time after treatment with U46619 (0.1 μM) with or without L670596 (1 μM) or Calp V (1 μM). Values are mean ± SEM of 3 experiments. * $P < 0.05$ compared to all other corresponding values.

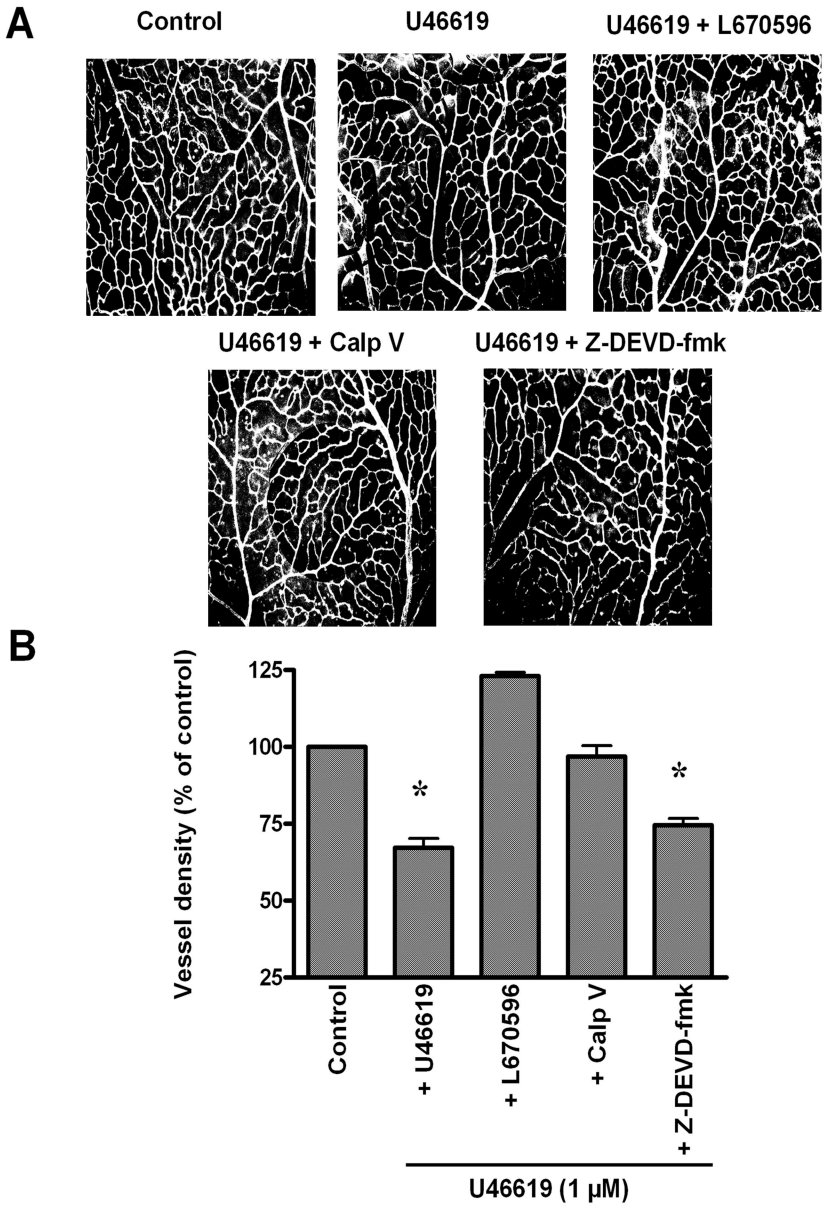
A
Control
U46619
U46619 + L670596
U46619 + Calp V
U46619 + Z-DEVD-fmk
B
Vessel density (% of control)
125
100
75
50
25
*
*
Control
+ U46619
+ L670596
+ Calp V
+ Z-DEVD-fmk
U46619 (1 μM)

Figure 1

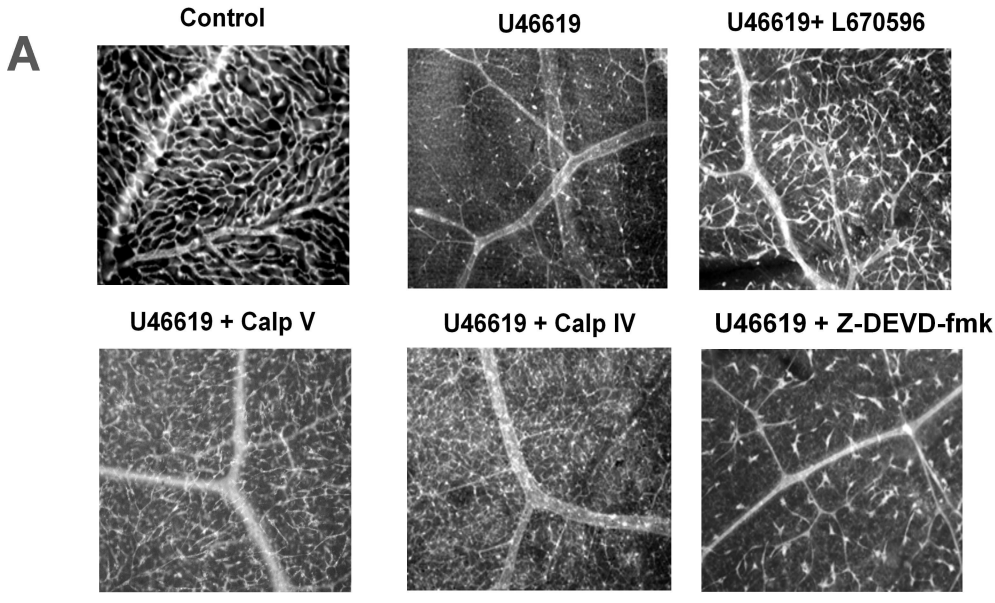
A
Control
U46619
U46619+ L670596
U46619 + Calp V
U46619 + Calp IV
U46619 + Z-DEVD-fmk
B
Vascular density (% of control)
100
75
50
*
*
Control
Vehicle
+ L670596
+ Calp IV
+ Calp V
+ Z-DEVD-fmk
U46619 (1 μM)

**Figure 2**

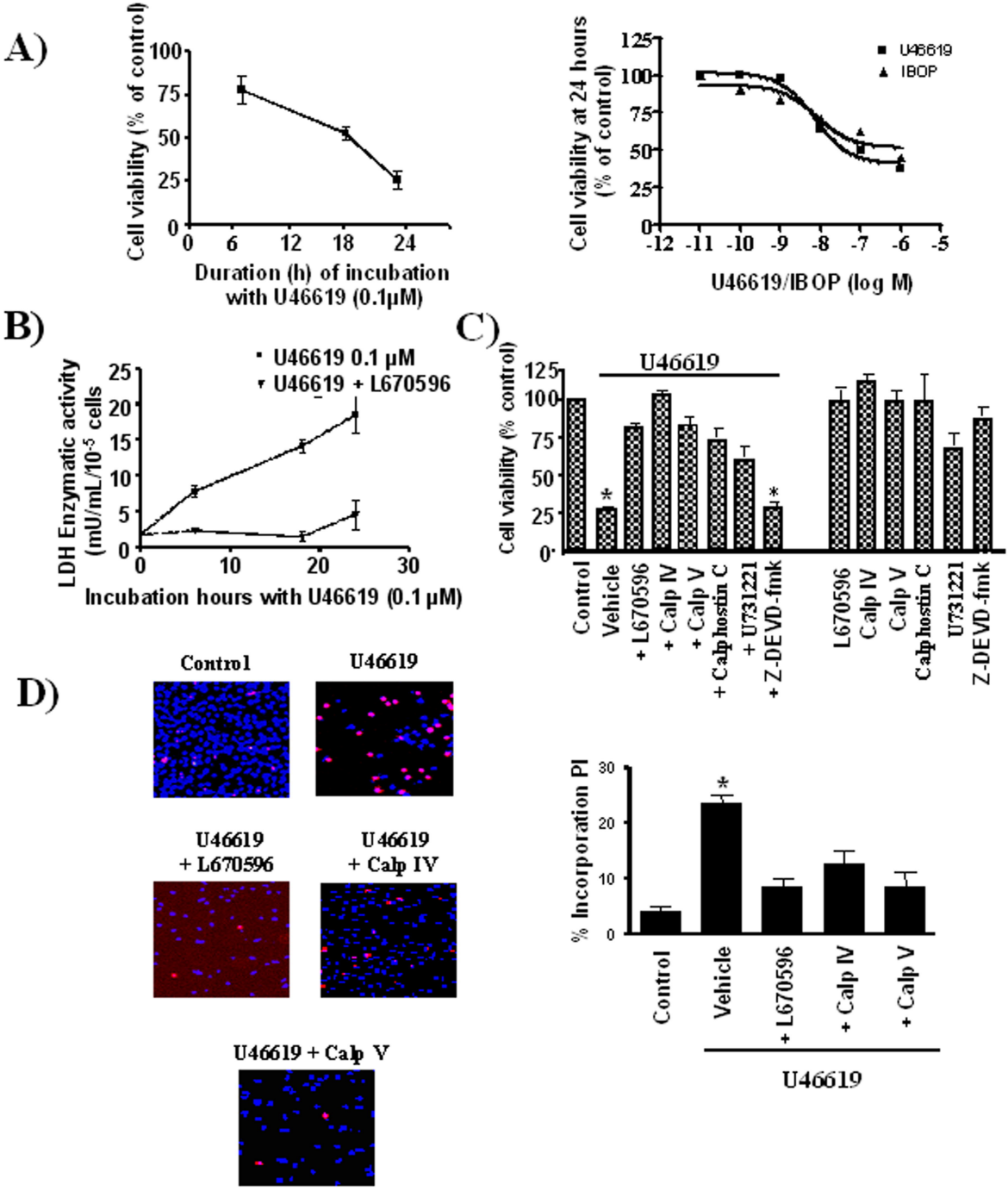
A)
Cell viability (% of control)
100
75
50
25
0
0 6 12 18 24
Duration (h) of incubation with U46619 (0.1μM)
Cell viability at 24 hours (% of control)
125
100
75
50
25
0
-12 -11 -10 -9 -8 -7 -6 -5
U46619
IBOP
U46619/IBOP (log M)
B)
U46619 0.1 μM
U46619 + L670596
LDH Enzymatic activity (mU/mL/10-5 cells)
25
20
15
10
5
0
0 10 20 30
Incubation hours with U46619 (0.1 μM)
C)
Cell viability (% control)
U46619
125
100
75
50
25
0
Control
Vehicle
+ L670596
+ Calp IV
+ Calp V
+ Calphostin C
+ U731221
+ Z-DEVD-fmk
L670596
Calp IV
Calp V
Calphostin C
U731221
Z-DEVD-fmk
D)
Control
U46619
U46619 + L670596
U46619 + Calp IV
U46619 + Calp V
% Incorporation PI
30
20
10
0
Control
Vehicle
+ L670596
+ Calp IV
+ Calp V
U46619

Figure 3

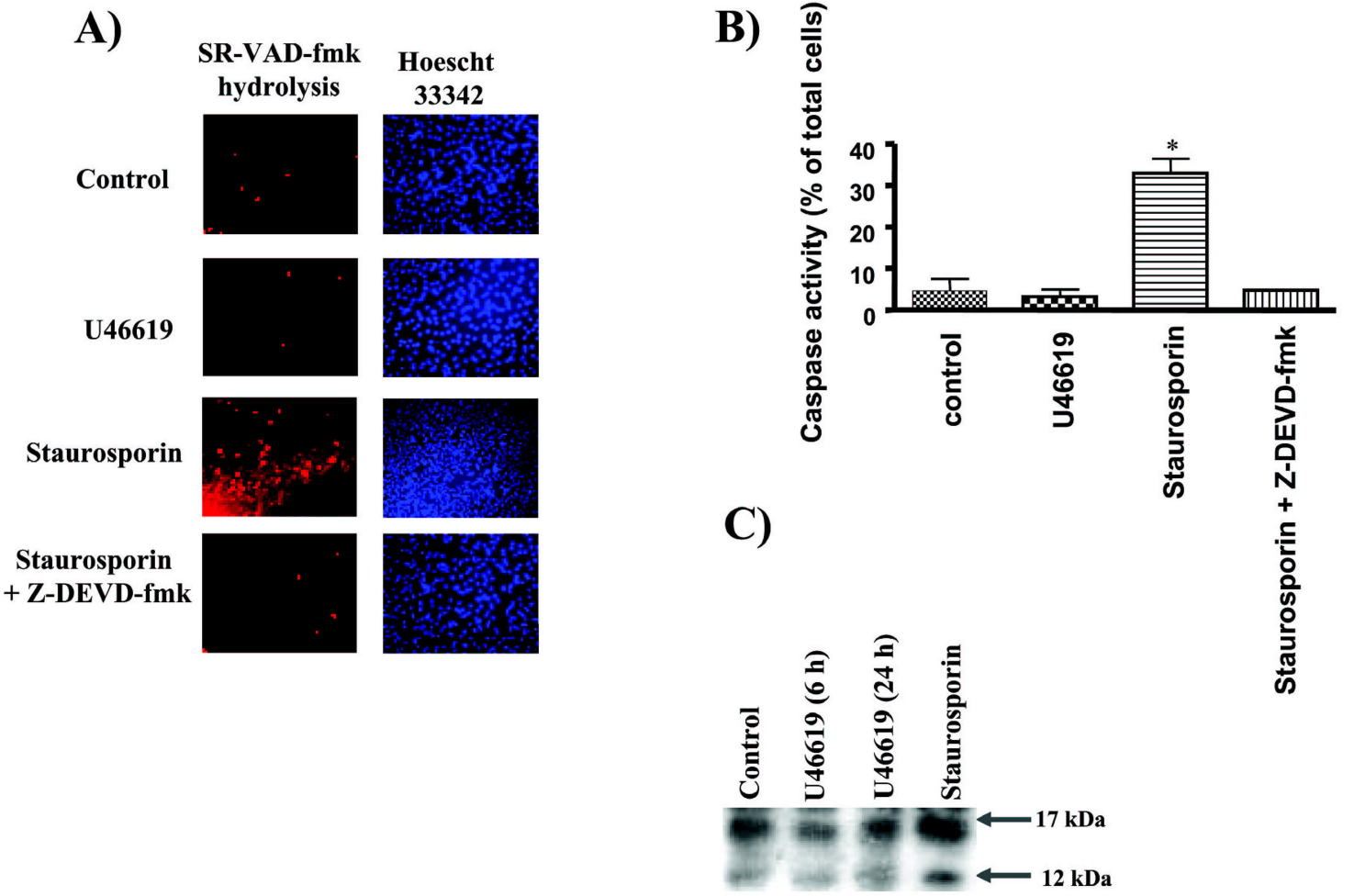
A)
SR-VAD-fmk hydrolysis
Hoescht 33342
Control
U46619
Staurosporin
Staurosporin + Z-DEVD-fmk
B)
Caspase activity (% of total cells)
40
30
20
10
0
*
control
U46619
Staurosporin
Staurosporin + Z-DEVD-fmk
C)
Control
U46619 (6 h)
U46619 (24 h)
Staurosporin
17 kDa
12 kDa

Figure 4

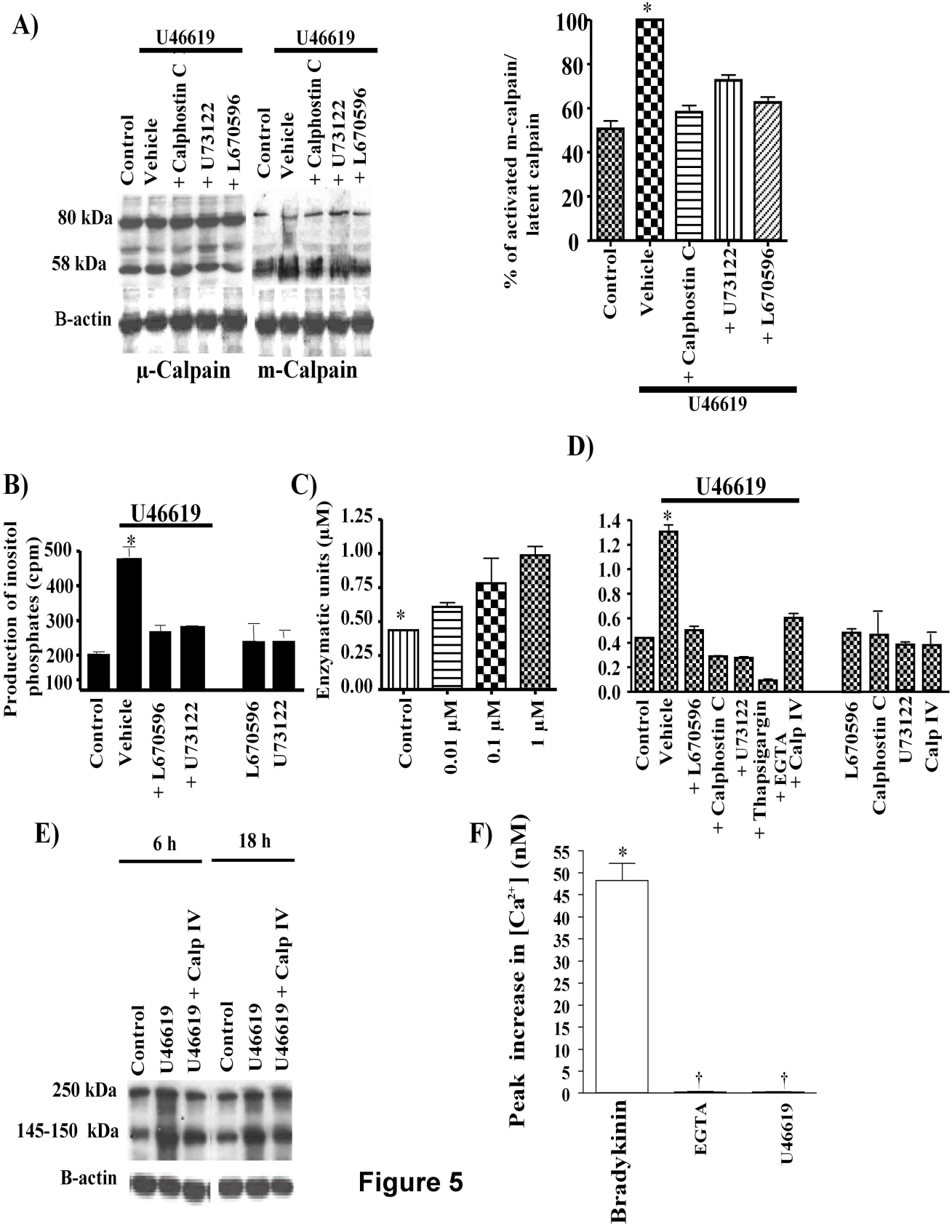
A)
U46619
U46619
Control
Vehicle
+ Calphostin C
+ U73122
+ L670596
Control
Vehicle
+ Calphostin C
+ U73122
+ L670596
80 kDa
58 kDa
B-actin
μ-Calpain
m-Calpain
% of activated m-calpain/ latent calpain
100
80
60
40
20
0
*
Control
Vehicle
+ Calphostin C
+ U73122
+ L670596
U46619
B)
U46619
Production of inositol phosphates (cpm)
500
400
300
200
100
*
Control
Vehicle
+ L670596
+ U73122
L670596
U73122
C)
Enzymatic units (μM)
1.25
1.00
0.75
0.50
0.25
0.00
*
Control
0.01 μM
0.1 μM
1 μM
D)
U46619
1.4
1.2
1.0
0.8
0.6
0.4
0.2
0.0
*
Control
Vehicle
+ L670596
+ Calphostin C
+ U73122
+ Thapsigargin
+ EGTA
+ Calp IV
L670596
Calphostin C
U73122
Calp IV
E)
6 h
18 h
Control
U46619
U46619 + Calp IV
Control
U46619
U46619 + Calp IV
250 kDa
145-150 kDa
B-actin
F)
Peak increase in [Ca2+] (nM)
55
50
45
40
35
30
25
20
15
10
5
0
*
†
†
Bradykinin
EGTA
U46619

Figure 5

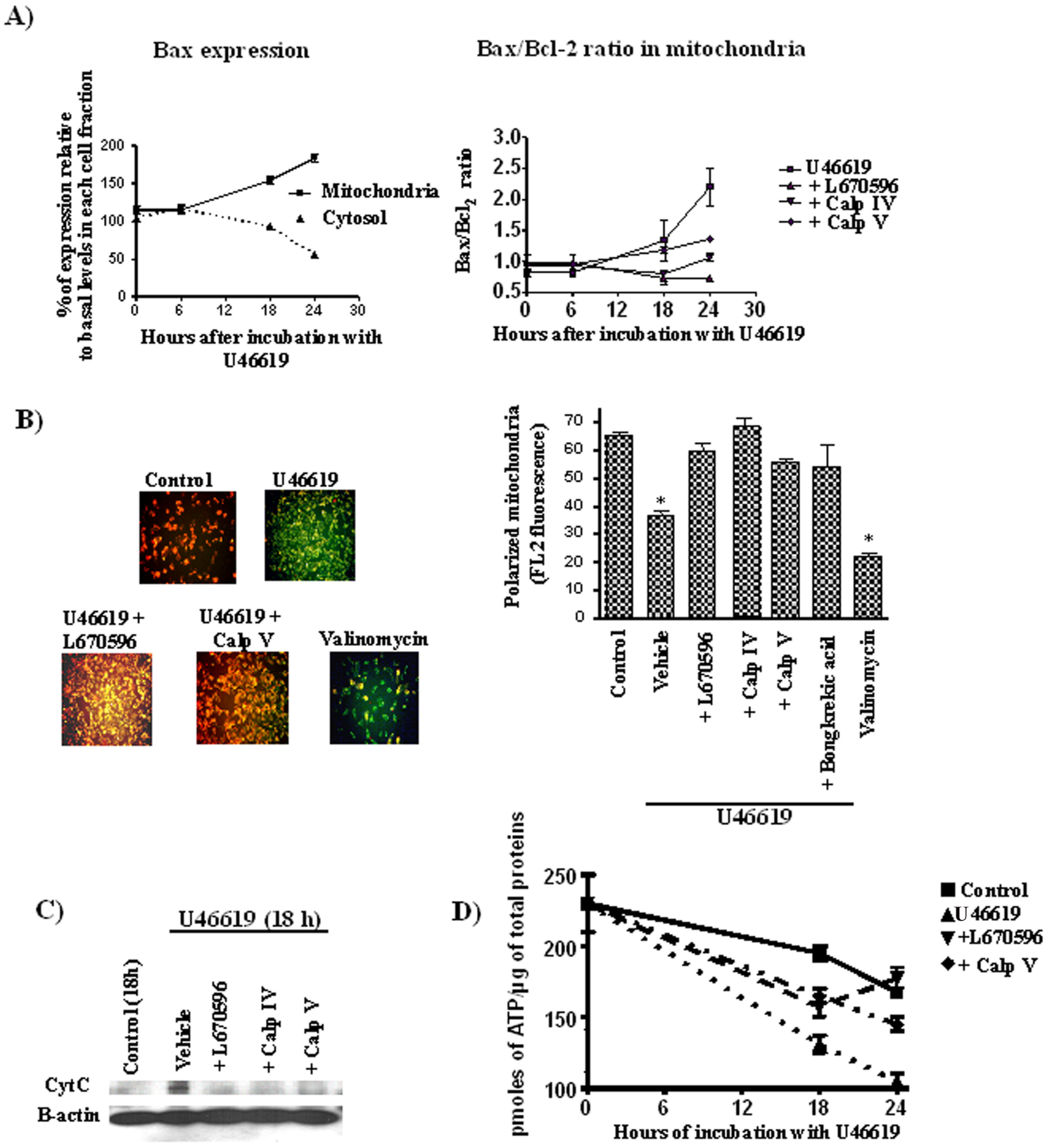
A)
Bax expression
% of expression relative to basal levels in each cell fraction
Mitochondria
Cytosol
Hours after incubation with U46619
Bax/Bcl-2 ratio in mitochondria
Bax/Bcl2 ratio
U46619
+ L670596
+ Calp IV
+ Calp V
Hours after incubation with U46619
B)
Control
U46619
U46619 + L670596
U46619 + Calp V
Valinomycin
Polarized mitochondria (FL2 fluorescence)
Control
Vehicle
+ L670596
+ Calp IV
+ Calp V
+ Bongkrekic acid
Valinomycin
U46619
C)
U46619 (18 h)
Control (18h)
Vehicle
+ L670596
+ Calp IV
+ Calp V
CytC
B-actin
D)
pmoles of ATP/µg of total proteins
Control
U46619
+L670596
+ Calp V
Hours of incubation with U46619

**Figure 6**